

## Ingestion kinetics of mixotrophic and heterotrophic flagellates

Kyle F. Edwards  <sup>1,\*</sup> Qian Li  <sup>1,2,3</sup> Grieg F. Steward  <sup>1,2</sup>

<sup>1</sup>Department of Oceanography, School of Ocean and Earth Science and Technology (SOEST), University of Hawai'i at Mānoa, Honolulu, USA

<sup>2</sup>Daniel K. Inouye Center for Microbial Oceanography: Research and Education, School of Ocean and Earth Science and Technology (SOEST), University of Hawai'i at Mānoa, Honolulu, USA

<sup>3</sup>School of Oceanography, Shanghai Jiao Tong University, Shanghai Shi, Xuhui Qu, China

### Abstract

In sunlit waters, significant predation is performed by unicellular, phagotrophic mixotrophs, that is, predators that also possess plastids. The success of a mixotrophic lifestyle will depend in part on how well mixotrophs acquire prey relative to specialized heterotrophs. Likewise, consequences of mixotrophy for productivity and element cycling will depend on the rate and efficiency at which mixotrophs consume prey biomass relative to heterotrophs. However, trait differences between mixotrophs and heterotrophs are not well characterized. In addition, cell size of mixotrophs varies widely, and constitutive mixotrophs include small flagellates deriving from diverse taxa, while larger species are primarily dinoflagellates. To determine whether similar constraints apply to phagotrophs across this broad range of size and taxa, we compiled 83 measurements of flagellate functional responses and compared maximum clearance rates ( $C_{\max}$ ) and maximum ingestion rates ( $I_{\max}$ ) between trophic modes. We found that the average mixotroph has a 3.7-fold lower  $C_{\max}$  and 7.8-fold lower  $I_{\max}$  than the average heterotroph, after controlling for cell size. The smaller penalty for  $C_{\max}$  suggests that relative fitness of mixotrophs will be enhanced under dilute prey concentrations that are common in pelagic ecosystems. We also find that growth efficiency is greater for mixotrophs and for flagellates with lower  $C_{\max}$ , indicating a spectrum of trophic strategies that may be driven by phototrophy vs. phagotrophy allocation as well as fast vs. slow metabolic variation. Allometric scaling shows that  $I_{\max}$  is constrained by a common relationship among dinoflagellates and other taxa, but dinoflagellates achieve a greater volume-specific  $C_{\max}$ . These results should aid in interpreting protistan communities and modeling mixotrophy.

Many of the diverse unicellular protists that inhabit sunlit waters are phagotrophic mixotrophs, possessing photosynthetic plastids while also ingesting prey (Stoecker et al. 2017). It is important to understand the environmental conditions that favor different forms of mixotrophy (Rothhaupt 1996; Ward et al. 2011; Leles et al. 2018; Edwards 2019), and the consequences of mixotrophy for ecosystem processes such as productivity, nutrient cycling, and carbon export (Mitra

et al. 2014; Ward and Follows 2016; Glibert and Mitra 2022). The causes and consequences of mixotrophy will depend strongly on the functional traits of mixotrophs, which can vary substantially across taxa. The relative fitness of mixotrophic strategies in different environments will depend on the rate at which they acquire resources (prey, dissolved nutrients, light), the efficiency with which they convert resources to new biomass, and how these traits differ for mixotrophs relative to autotrophs and heterotrophs. Competition for prey between mixotrophs and heterotrophs will depend on the extent to which ingestion rates are lower for the generalized mixotrophs relative to specialized heterotrophs, caused by allocation of energy and/or biomass toward phototrophy (Raven 1997; Berge et al. 2016). At the same time, the energy subsidy from photon capture may allow mixotrophs to suppress prey to a lower concentration even if ingestion rates are lower (Rothhaupt 1996). These trait differences will have ecosystem consequences, because mixotrophs should transfer more prey carbon and nutrients up food chains, if their energy demands are met by absorbed light

\*Correspondence: [kfe@hawaii.edu](mailto:kfe@hawaii.edu)

This is an open access article under the terms of the [Creative Commons Attribution-NonCommercial-NoDerivs](#) license, which permits use and distribution in any medium, provided the original work is properly cited, the use is non-commercial and no modifications or adaptations are made.

Additional Supporting Information may be found in the online version of this article.

**Author Contribution Statement:** All authors contributed to study conceptualization and manuscript writing, and have approved the final manuscript. K.F.E. compiled and analyzed the data.

rather than respiration of prey biomass (Mitra et al. 2014; Ward and Follows 2016). The magnitude of this effect will itself depend on ingestion kinetics and the relative competitive success (abundance) of mixotrophs, which will determine what fraction of prey biomass is channeled through mixotroph vs. heterotroph consumers.

Phagotrophic mixotrophs can be divided into constitutive mixotrophs, which create/inherit their own plastids, and non-constitutive mixotrophs, which sequester plastids from their prey or harbor endosymbiotic photosynthesizers (Mitra et al. 2016). Constitutive mixotrophy occurs in many eukaryotic lineages, but these organisms of diverse origin are united by having a flagellate morphology in nearly all cases (Stoecker et al. 2017). In contrast, the non-constitutive mixotrophs include flagellates, ciliates, and various amoeboid protists from the phylum Rhizaria (Stoecker et al. 2017). Among constitutive mixotrophs in the ocean, smaller forms ( $\sim 10 \mu\text{m}$  equivalent spherical diameter) come from many ancient lineages, including haptophytes, chrysophytes, cryptophytes, dictyochophytes, dinoflagellates, bolidophytes, chlorophytes, chorarachniophytes, and others (Pierella Karlusich et al. 2020). In contrast, mixotrophic flagellates  $> 10 \mu\text{m}$  appear to be largely dinoflagellates. A similar pattern may hold for heterotrophic flagellates as well, with smaller forms coming from a variety of clades, many of which remain uncultured (Logares et al. 2012), while dinoflagellates prevail in the larger size class (Arndt et al. 2000).

Ingestion rates of flagellates and other predators commonly exhibit a hyperbolic functional response (Holling 1966; Hansen et al. 1997), which can be characterized by two parameters: the maximum clearance rate ( $C_{\max}$ ), which is the initial slope of the curve, and the maximum ingestion rate ( $I_{\max}$ ), which is the asymptote (Kiørboe 2008).  $C_{\max}$  is expected to determine competition for prey in most situations, because biomass in pelagic ecosystems is dilute (Kiørboe 2008), and because competition tends to deplete resources to low concentrations. In contrast,  $I_{\max}$  will determine relative success under relatively high prey concentrations, which may be found in episodic blooms, or particle-associated microbial hotspots (Azam et al. 1994). A previous study measured and compiled  $C_{\max}$  and  $I_{\max}$  estimates of a variety of mixotrophic and heterotrophic nanoflagellates, and it was noted that  $C_{\max}$  values broadly overlapped between the trophic modes, while  $I_{\max}$  tended to be lower for mixotrophs. However, no quantitative comparisons between trophic modes (i.e., mixotrophs and heterotrophs) were performed, and it is unknown how the magnitude of any differences compares to that seen in larger flagellates. This study also found that mixotrophs with faster clearance rates tended to have lower growth efficiency, which could be caused by relatively autotrophic mixotrophs possessing both lower ingestion rates and less respiration of prey biomass. The growth efficiency of mixotrophs could have large effects on ecosystem trophic transfer efficiency and nutrient cycling (Leles et al. 2018), but

it is unknown how the growth efficiencies of these mixotrophs compare to heterotrophs as well as other mixotrophs. Finally, a compilation of dinoflagellate experiments found lower  $I_{\max}$  and lower maximum growth rates of mixotrophic dinoflagellates compared to heterotrophs (Jeong et al. 2010), but  $C_{\max}$  was not analyzed.

In this study, we synthesize a large number of experiments that used flagellate cultures to measure ingestion kinetics and growth. The goal is to gain insight into the tradeoffs affecting constitutive mixotrophs, the diversity of traits among mixotrophs and heterotrophs, and whether similar constraints apply to the diverse smaller flagellates and the larger dinoflagellates.

## Methods

### Data compilation

The literature was comprehensively searched for lab experiments that measured the functional response (ingestion rate vs. prey concentration) of flagellates. This yielded 83 experiments from 57 publications (Supporting Information Table S1), resulting in data for 23 heterotrophic non-dinoflagellates (equivalent spherical diameter [ESD] range 3–9  $\mu\text{m}$ ), 16 mixotrophic non-dinoflagellates (ESD range 2.2–17  $\mu\text{m}$ ), 22 heterotrophic dinoflagellates (ESD range 5.3–73  $\mu\text{m}$ ), and 22 mixotrophic dinoflagellates (ESD range 4–55  $\mu\text{m}$ ). Some of these studies were compiled in previous syntheses (Hansen et al. 1997; Jeong et al. 2010), but for consistency all data were collected anew from the original publications. In nearly all cases, estimates of  $C_{\max}$  and  $I_{\max}$  were reported in the original publication, from a fitted type II functional response:  $I = \frac{C_{\max}P}{1 + \frac{C_{\max}}{I_{\max}}P}$  where  $I$  is ingestion rate (prey cells per flagellate per time),  $P$  is prey concentration (cells per volume), and  $C_{\max}$  has units of volume per flagellate per time. In a minority of cases the raw data were extracted from figures using Datathief (Tummers 2006), and a type II functional response was fit using maximum likelihood, with the R package bbmle (Bolker and R Development Core Team 2022). In three cases, the prey concentrations tested did not begin to saturate ingestion rate, and so  $C_{\max}$  (the initial slope of the functional response) was calculated, but not  $I_{\max}$  (the asymptote). From studies where the functional response was measured using multiple prey types, we recorded only the parameter estimates from the prey that yielded the fastest predator growth. The study reported functional response parameters for six mixotrophic flagellates; we also included four additional estimates of  $C_{\max}$  (but not  $I_{\max}$ ) from experiments where clearance rate was measured over a range of prey concentrations that were too low to saturate ingestion.

Measurements of flagellate volume and prey volume were also extracted from the original studies, as well as culture temperature. From studies where flagellate volume was measured over a range of prey concentrations, we recorded the volume at low concentration for analysis of  $C_{\max}$  relationships and

the volume at high concentration for analysis of  $I_{\max}$ . From studies that measured flagellate growth rate vs. prey concentration, we also extracted the maximum growth rate,  $\mu_{\max}$  (i.e., the asymptote of the relationship). The value for  $\mu_{\max}$  was used to calculate the growth efficiency, in biovolume units, at high prey concentration:  $\mu_{\max} \frac{V_F}{I_{\max} V_p}$ , where  $V_p$  is prey cell volume and  $V_F$  is flagellate volume. This quantity is the maximum growth rate divided by the volume-specific maximum ingestion rate ( $\frac{I_{\max} V_p}{V_F}$ , volume of prey cells ingested per flagellate volume per time), and it estimates growth efficiency as the specific rate of increase of flagellate cells relative to the specific rate of ingestion. Although it would be preferable to measure growth efficiency in biomass units or carbon mass units, elemental composition was not measured in most of the compiled studies, and the biovolume-based efficiency provides an index that can be compared across a large fraction of the experiments. To facilitate comparison between dinoflagellate mixotrophs and non-dinoflagellate mixotrophs, we also included biovolume growth efficiencies, where this quantity was estimated as the total volume of flagellate cells produced relative to the total volume of prey cells consumed in the same experiments used to measure ingestion rates.

### Statistical analysis

To compare the traits of mixotrophic and heterotrophic flagellates, we used linear models where log-transformed trait values were the response variables and the predictors included trophic mode (mixotroph/heterotroph), log flagellate volume, and taxonomy (dinoflagellate/non-dinoflagellate), as well as the two-way interactions between these predictors. In R syntax the model is  $\log_{10}(\text{Trait}) \sim \log_{10}(\text{volume}) + \text{trophic.mode} + \text{taxonomy} + \text{trophic.mode:taxonomy} + \text{trophic.mode:log}_{10}(\text{volume}) + \text{taxonomy:log}_{10}(\text{volume})$ . A linear log-log relationship between a trait and body volume is equivalent to a power law, which is commonly used to estimate allometric scaling relationships. Therefore, the linear models are estimating  $T = aV^b$ , where  $T$  is the trait of interest,  $V$  is cell volume,  $a$  determines the overall height of the curve, and  $b$  is the scaling exponent. In the linear model, the intercept is equal to  $\log_{10}(a)$  and the slope for  $\log_{10}(\text{volume})$  is equal to  $b$ . The term “trophic.mode” tests whether  $\log_{10}(a)$  differs between mixotrophs and heterotrophs, the term “taxonomy” tests whether  $\log_{10}(a)$  differs between dinoflagellates and non-dinoflagellates, the term “trophic.mode:taxonomy” tests whether the difference between mixotrophs and heterotrophs in  $\log_{10}(a)$  changes between dinoflagellates and non-dinoflagellates, the term “trophic.mode:log<sub>10</sub>(volume)” tests whether  $b$  differs between mixotrophs and heterotrophs, and the term “taxonomy:log<sub>10</sub>(volume)” tests whether  $b$  differs between dinoflagellates and non-dinoflagellates. The taxonomy of the non-dinoflagellates was not included in the models because high diversity limited taxon-level replication, and we were primarily interested in

whether the larger dinoflagellates exhibited different patterns from the other flagellates. Temperature was examined as a predictor, but it never explained significant variation and for brevity will not be reported in the “Results” section. In addition to the model structure described above, we allowed the residual trait variation to vary by trophic mode and taxonomy as a way of comparing the trait variance between mixotrophs and heterotrophs while controlling for cell size. Significance of all model terms was assessed with marginal chi-squared likelihood ratio tests, and non-significant interactions were dropped in order to choose the best model for visualization and reporting of scaling relationships.

We performed a set of sensitivity analyses to assess the robustness of the statistical results. (1) Instead of incorporating experimental temperature as a predictor, we corrected all traits for varying temperature by assuming a  $Q_{10}$  of 2.8 (Hansen et al. 1997). (2) Because the smallest dinoflagellate (*Pelagodinium*) has a very low  $C_{\max}$ , we assessed the effect of removing it. (3) Because the size range of mixotrophs and heterotrophs is somewhat different, we assessed the effect of only including flagellates between 3 and 54.5  $\mu\text{m}$ , which excludes the two smallest and two largest species. (4) Finally, we assessed the effect of adding a random effect for the publication in which data were reported, because methods used in a study on multiple species could shift their trait values in a similar way.

All models were fit in R with the package glmmTMB (Brooks et al. 2022), which was utilized because it readily incorporates residual variances that vary between groups, as well as random effects if needed. The dataset and R code are included as supplementary files.

## Results

### Maximum clearance rate

$C_{\max}$  varied by five orders of magnitude, with half of this variation explained by flagellate size, trophic mode, and taxonomy (model  $R^2 = 0.50$ ; Figs. 1a, 2a). The slope of the log-log relationship between  $C_{\max}$  and cell volume, which is equivalent to the exponent of a power-law relationship, is 0.38 (95% confidence interval [CI]: [0.19, 0.58];  $\chi^2_1 = 12$ ,  $p < 10^{-3}$ ; Table 1). This slope does not differ significantly between mixotrophs and heterotrophs ( $\chi^2_1 = 0.05$ ,  $p = 0.82$ ) or between dinoflagellates and non-dinoflagellates ( $\chi^2_1 = 2.4$ ,  $p = 0.12$ ).  $C_{\max}$  values of mixotrophs and heterotrophs overlap considerably, but their intercepts are significantly different, with mixotrophs on average having a 3.7-fold lower  $C_{\max}$  than heterotrophs of the same size ( $\chi^2_1 = 12$ ,  $p < 10^{-3}$ ; Table 1). Dinoflagellates have a  $C_{\max}$  that is 16-fold higher than that expected for non-dinoflagellates of the same size ( $\chi^2_1 = 26$ ,  $p < 10^{-6}$ ; Table 1). The difference in  $C_{\max}$  between mixotrophs and heterotrophs is of similar magnitude for both dinoflagellates and non-dinoflagellates ( $\chi^2_1 = 0.03$ ,  $p = 0.87$ ). Sensitivity

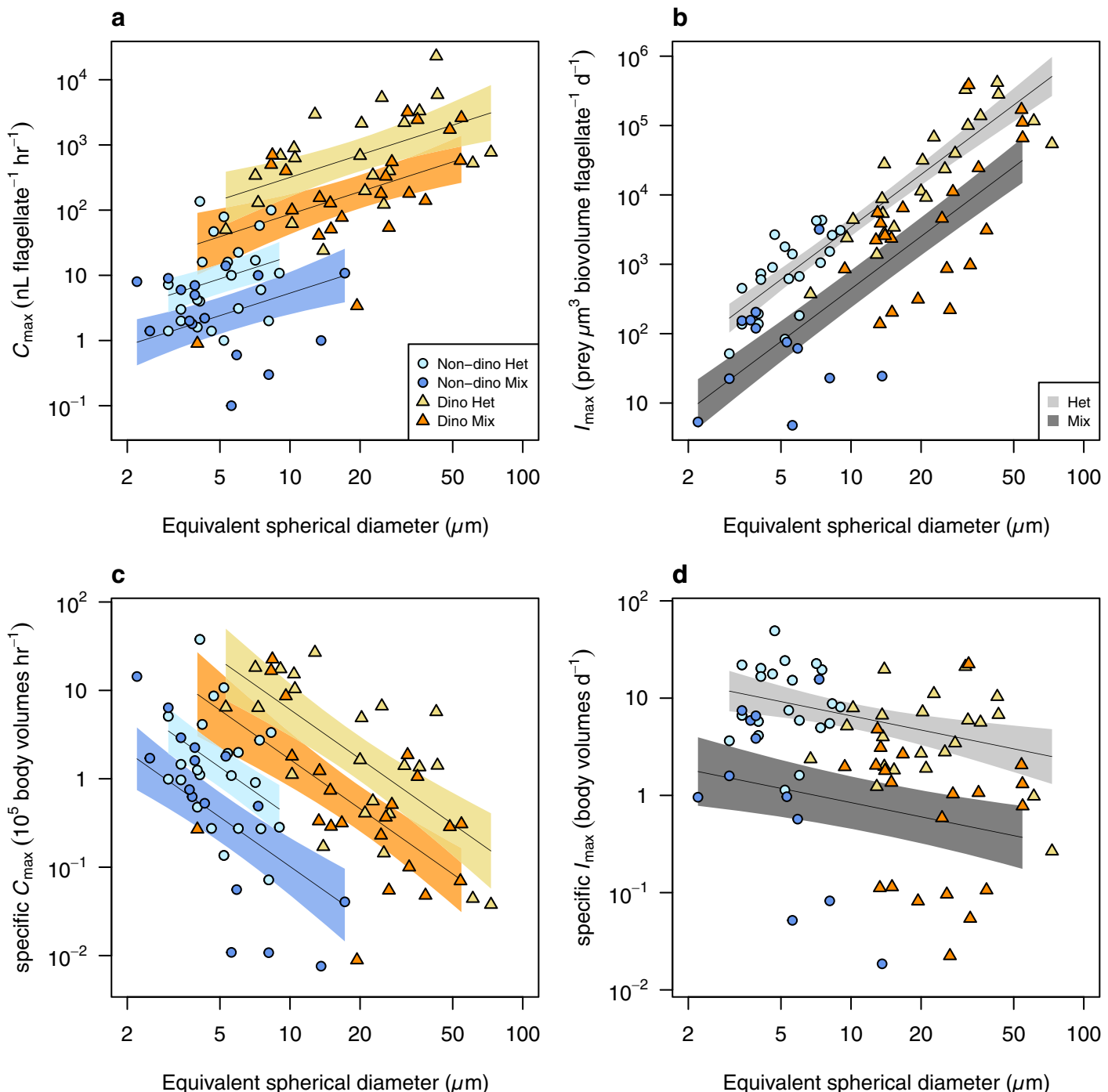


**Fig. 1.** Maximum clearance rate and maximum ingestion rate of mixotrophic and heterotrophic flagellates. **(a)** Maximum clearance rate vs. flagellate size, **(b)** maximum ingestion rate vs. flagellate size, **(c)** volume-specific maximum clearance rate vs. flagellate size, **(d)** volume-specific maximum ingestion rate vs. flagellate size. Lines and shaded intervals are from the statistical models best supported by the data. In **(a)** and **(c)**, the intercept varies by trophic mode and taxonomy, while the slope is common across these groups. In **(b)** and **(d)**, the intercept varies by trophic mode, while the slope is common across these groups.

analyses did not qualitatively change any of the reported hypothesis tests, and generally had small effects on parameter estimates, although removing the small dinoflagellate *Pelagodinium* decreases the allometric scaling exponent (0.31

instead of 0.38), and removing the smallest two and largest two flagellates increases the scaling exponent (0.48 vs. 0.38), shifts which are within the original 95% CI of [0.19, 0.58] (Supporting Information Table S2).

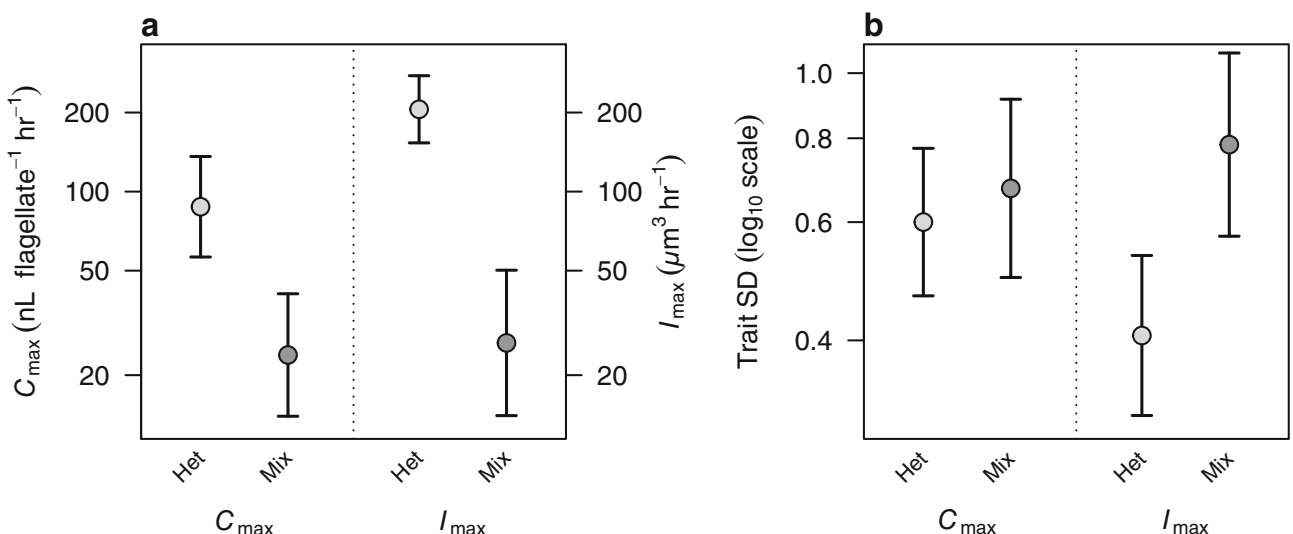


**Fig. 2.** Model-fitted differences between mixotrophs and heterotrophs. **(a)** Predicted  $C_{\max}$  and  $I_{\max}$  for heterotrophic and mixotrophic flagellates of average size ( $\sim 11 \mu\text{m}$  equivalent spherical diameter). Because the model is fit to  $\log_{10}$ -transformed trait values, the proportional trait difference between heterotrophs and mixotrophs is constant across flagellate sizes (3.7-fold for  $C_{\max}$  and 7.8-fold for  $I_{\max}$ ). **(b)** Residual standard deviation of  $C_{\max}$  and  $I_{\max}$ . Because the model was fit to  $\log_{10}$ -transformed trait values, the standard deviations do not depend on trait units and are directly comparable between traits (e.g., a SD of 0.4 means that a trait value typically differs from the mean by a factor of  $10^{0.4} = 2.5$ ). Errors bars are 95% confidence intervals.

### Maximum ingestion rate

Similar to  $C_{\max}$ ,  $I_{\max}$  varies by five orders of magnitude, with half of this variation explained by flagellate size and trophic mode (model  $R^2 = 0.50$ ; Figs. 1b, 2a). The slope of the log-log relationship between  $I_{\max}$  and cell volume is 0.84 (95% CI: [0.67, 1.0];  $\chi^2 = 110$ ,  $p < 10^{-15}$ ; Table 1), and this slope is significantly steeper than the slope for  $C_{\max}$  ( $\chi^2 = 15$ ,  $p < 10^{-4}$ ). The slope does not differ significantly between mixotrophs and heterotrophs ( $\chi^2 = 0.88$ ,  $p = 0.35$ ) or between dinoflagellates and non-dinoflagellates ( $\chi^2 = 0.0003$ ,  $p = 0.99$ ). On average mixotrophs have an  $I_{\max}$  that is 7.8 times less than heterotrophs of the same size ( $\chi^2 = 26$ ,  $p < 10^{-6}$ ; Table 1), and this difference is greater than the difference in  $C_{\max}$  between mixotrophs and heterotrophs ( $\chi^2 = 6.6$ ,  $p = 0.01$ ). Unlike the pattern for  $C_{\max}$ ,  $I_{\max}$  does not differ between dinoflagellate and non-dinoflagellates ( $\chi^2 = 0.002$ ,  $p = 0.97$ ). The difference in  $I_{\max}$  between mixotrophs and

heterotrophs does shift significantly between dinoflagellates and non-dinoflagellates ( $\chi^2 = 1.2$ ,  $p = 0.28$ ). Sensitivity analyses did not qualitatively change any of the reported hypothesis tests, and generally had small effects on parameter estimates, although removing the smallest two and largest two flagellates increases the scaling exponent to 1.0, which is within the original 95% CI of [0.67, 1.0] (Supporting Information Table S2).

### Trait variances

Variation in  $C_{\max}$  is slightly greater for mixotrophs (SD = 0.67) compared to heterotrophs (SD = 0.60), but the difference is not significant ( $\chi^2 = 0.47$ ,  $p = 0.49$ ; Fig. 2b). Because the traits are analyzed on a log<sub>10</sub> scale, an SD of 0.67 means that on average the value for a particular mixotroph differs from the mean value for that cell size by a factor of  $10^{0.67} = 4.7$ . For a heterotroph this is a factor of  $10^{0.60} = 4$ .

**Table 1.** Allometric scaling of ingestion parameters. For  $C_{\max}$  and  $I_{\max}$  the model estimates for the relationship Trait =  $aV^b$  are taken from the best-fit statistical models (Fig. 1), which have common slopes ( $b$ ) across groups but distinct intercepts ( $a$ ). Numbers are point estimates with 95% confidence intervals in parentheses. Units for  $C_{\max}$  are nL predator $^{-1}$  h $^{-1}$  and for  $I_{\max}$  are prey  $\mu\text{m}^3$  biovolume predator $^{-1}$  d $^{-1}$ .

	$C_{\max}$	$I_{\max}$
<i>a</i>	Non-dinoflagellate mixotrophs	0.48 (0.17, 1.4)
	Dinoflagellate mixotrophs	7.8 (1.4, 43)
	Non-dinoflagellate heterotrophs	1.8 (0.68, 4.6)
	Dinoflagellate heterotrophs	29 (5.4, 150)
<i>b</i>	All groups	0.38 (0.19, 0.58)
		All groups
		0.84 (0.67, 1.0)

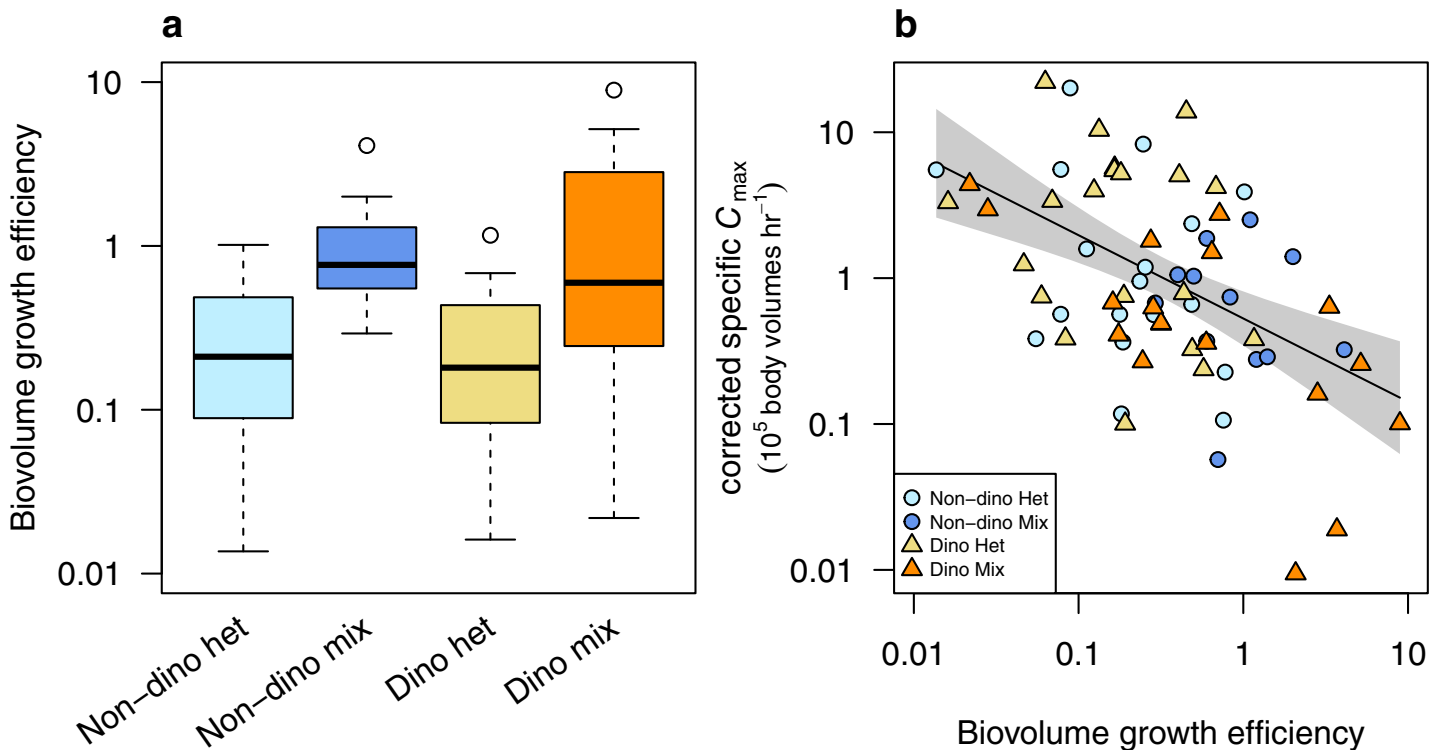


**Fig. 3.** (a) Biovolume-based growth efficiency of mixotrophic and heterotrophic flagellates. (b) Corrected specific  $C_{\max}$  vs. growth efficiency. The correction uses a statistical model to remove effects of flagellate size and taxonomy (dinoflagellate vs. non-dinoflagellate), to illustrate the magnitude of covariation between specific  $C_{\max}$  and growth efficiency when the other variables are held constant.

For  $I_{\max}$  the variation among the mixotrophs ( $SD = 0.78$ , or a factor of 6) is greater than the variation among the heterotrophs ( $SD = 0.4$ , or a factor of 2.5;  $\chi^2 = 16$ ,  $p < 10^{-4}$ ; Fig. 2b). As a result, the amount of variation in  $C_{\max}$  and  $I_{\max}$  is comparable for the mixotrophs, but for heterotrophs  $C_{\max}$  is more variable than  $I_{\max}$ . Neither of these traits differs in variability between dinoflagellates and non-dinoflagellates ( $C_{\max}$ :  $\chi^2 = 0.12$ ,  $p = 0.73$ ;  $I_{\max}$ :  $\chi^2 = 0.0007$ ,  $p = 0.98$ ).

#### Volume-specific ingestion parameters

The allometric relationships between  $C_{\max}$  and cell volume, and between  $I_{\max}$  and cell volume, both have slopes  $< 1$ , which implies that the same ingestion parameters measured in volume-specific units tend to decline with cell size. This is observed when volume-specific parameters are calculated (Fig. 1c,d). The slope for specific  $C_{\max}$  vs. cell volume is  $-0.62$  (95% CI:  $[-0.81, -0.42]$ ) and the slope for  $I_{\max}$  vs. cell volume is  $-0.16$  (95% CI:  $[-0.26, -0.06]$ ). Estimation of these slopes is problematic, because flagellate volume is both a predictor in the model and a component of the response variable (i.e., it is in the denominators of specific  $C_{\max}$  and specific  $I_{\max}$ ). This means that measurement error in cell volume will tend to bias the slope to be more negative than the true value. Nonetheless, the values of these slopes are consistent with the expectation from the models displayed in

Fig. 1a,b: a slope of 0.38 for  $C_{\max}$  (Fig. 1a) predicts a slope of  $0.38 - 1 = -0.62$  for specific  $C_{\max}$ , and a slope of 0.84 for  $I_{\max}$  (Fig. 1b) predicts a slope of  $0.84 - 1 = -0.16$  for specific  $I_{\max}$ . Finally, the proportional differences between mixotrophs and heterotrophs, and between dinoflagellates and non-dinoflagellates, are the same when modeled using volume-specific parameters instead of the original parameters: for specific  $C_{\max}$ , a 3.7-fold difference for between heterotrophs and mixotrophs and a 16-fold difference between dinoflagellates and non-dinoflagellates; for specific  $I_{\max}$ , a 7.8-fold difference between heterotrophs and mixotrophs (Fig. 1c,d, statistical results not shown).

#### Growth efficiency

Growth efficiency measured in biovolume units (flagellate biovolume created per prey biovolume consumed) is greater for mixotrophs (geometric mean: 0.69) than for heterotrophs (geometric mean: 0.2; Fig. 3a;  $F_{1,63} = 13$ ,  $p < 10^{-3}$ ). Efficiency does not differ on average between dinoflagellate and non-dinoflagellates ( $F_{1,63} = 0.03$ ,  $p = 0.87$ ), and the difference between mixotrophs and heterotrophs does not differ between dinoflagellates and non-dinoflagellates ( $F_{1,63} = 0.01$ ,  $p = 0.90$ ). Growth efficiency of the mixotrophs may be biased upwards in this comparison because some experiments included dissolved nutrients in the culture medium, which could be used to

synthesize new biomass. However, the 10 efficiency estimates taken, from experiments with diverse small mixotrophs where dissolved nitrogen was not added, have a geometric mean of 0.98, suggesting that the substantially greater growth efficiency of mixotrophs is robust. When growth efficiency is added to a regression model for  $C_{\max}$  that includes cell size, taxonomy, and temperature as predictors, it explains significant additional variation, indicating that flagellates with greater growth efficiency tend to have lower maximum clearance rates ( $\chi^2_1 = 18, p < 10^{-4}$ ; partial correlation  $r = -0.52$ ; Fig. 3b). Growth efficiency remains as a significant predictor when only analyzing the mixotrophs ( $\chi^2_1 = 18, p < 10^{-3}$ ) or the heterotrophs ( $\chi^2_1 = 4.6, p < 0.03$ ), although the correlation is stronger within the mixotrophs (partial correlation  $r = -0.56$  for mixotrophs and  $r = -0.33$  for heterotrophs).

## Discussion

The experiments compiled in this study show that, on average, mixotrophic flagellates ingest prey at a slower rate than heterotrophs. The magnitude of this difference changes with prey concentration—the 3.7-fold difference in  $C_{\max}$  determines relative rates under non-saturating prey concentrations, and this approximately doubles to 7.8-fold under saturating prey concentrations where  $I_{\max}$  determines the functional response (Fig. 4a). The magnitude of these effects does not differ between the diverse nanoflagellates and the (mostly) larger dinoflagellates,

suggesting common underlying tradeoffs affecting mixotrophy across taxa.  $C_{\max}$  is highly variable, both within mixotrophs and within heterotrophs, while  $I_{\max}$  is more than twice as variable within mixotrophs compared to heterotrophs (Fig. 2). Some of the variation in these traits may be associated with physiological strategies that also affect growth efficiency, because  $C_{\max}$  is negatively correlated with growth efficiency, indicating that faster grazers exhibit lower efficiency (Fig. 3b). Some of the observed variation in ingestion traits is likely caused by variation in experimental conditions such as irradiance and nutrient concentrations. Ingestion rates of some mixotrophs have been shown to be stimulated by dissolved nutrient limitation (Smalley et al. 2003; Li et al. 2021), and ingestion can be positively or negatively correlated with irradiance (Stoecker 1998). Because the mean differences reported here average over a wide diversity of species and experiments, they should be relatively robust, but how mixotrophs and heterotrophs differ in situ will likely vary as species acclimate to different conditions, and as conditions select for particular species and genotypes. For example, mixotrophs with faster clearance rates become relatively more abundant in stratified waters with lower Chl *a*, and at shallower depths (Edwards et al. 2023), which could lead to smaller differences between mixotrophs and heterotrophs in ingestion rates. One limitation of the current study is that most of the small mixotrophs were isolated from the oligotrophic North Pacific Subtropical Gyre, while the small heterotrophs appear to be largely coastal in origin. Future work should endeavor to isolate

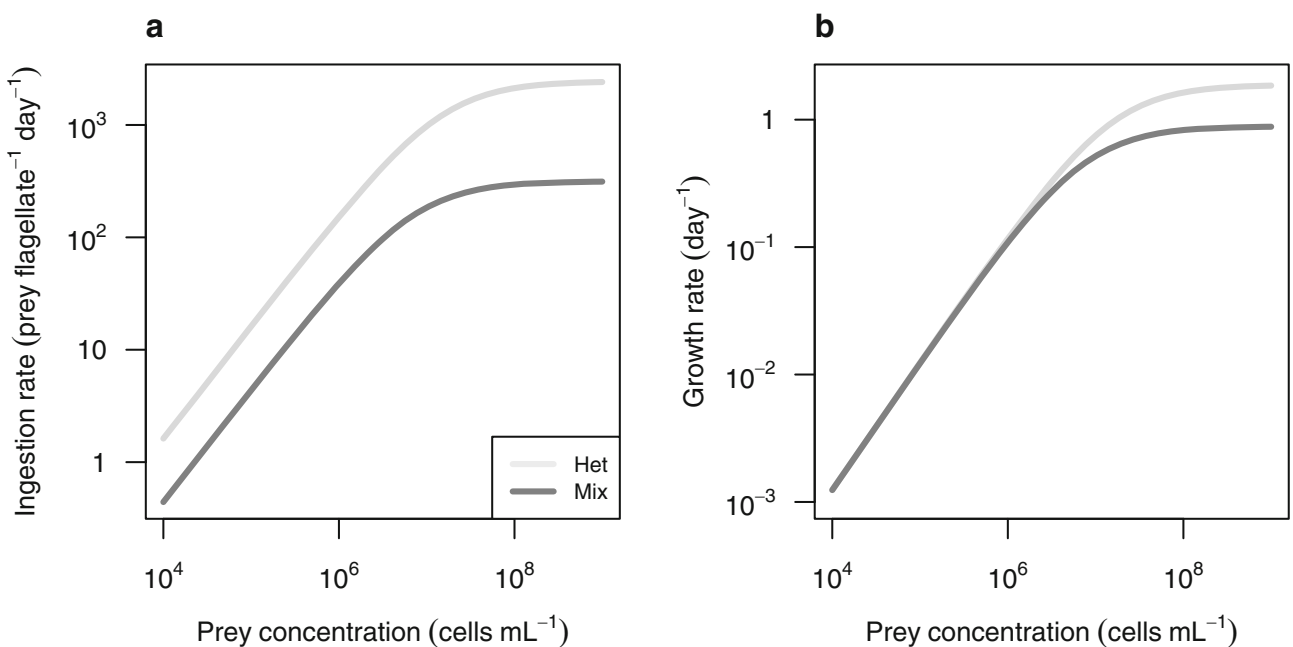


**Fig. 4.** Illustration of typical trait differences between heterotrophic and mixotrophic flagellates. (a) Functional response (ingestion rate vs. prey concentration), using average  $C_{\max}$  and  $I_{\max}$  values for a 4  $\mu\text{m}$  diameter flagellate consuming 0.64  $\mu\text{m}$  diameter prey (representing small flagellates consuming *Prochlorococcus*). (b) Growth rate vs. prey concentration, predicted using the functional responses multiplied by the average biovolume growth efficiencies of heterotrophic and mixotrophs. Choosing a flagellate or prey of different size would change the scales of the y- and x-axes but not the proportional differences between heterotroph and mixotroph curves.

and study the most abundant open ocean heterotrophic flagellates, which may be particularly well adapted to low prey concentrations, and compare them to co-occurring mixotrophs under uniform conditions.

### Implications for mixotroph ecology

One of the fundamental questions in mixotroph ecology is how environmental conditions combine with underlying tradeoffs to determine the success of different mixotrophic strategies, relative to autotrophs and heterotrophs. The fact that mixotrophs appear to suffer a smaller penalty for  $C_{\max}$  compared to  $I_{\max}$  implies that their ability to compete with heterotrophs for prey will be greater under lower prey density. It has also been argued on biophysical grounds that mixotrophs should suffer a lower nutrient uptake penalty, relative to autotrophs, when nutrients are scarce (Ward et al. 2011). This is because fewer nutrient transporters at the cell surface are needed to optimize uptake when the uptake rate is more susceptible to diffusion limitation (Lindemann et al. 2016). Therefore, mixotrophic strategies may experience the lowest costs when both prey and nutrients are at relatively low concentrations. Previous modeling work, with some experimental support, has shown that the success of a mixotrophic strategy depends on the supply ratio of prey and nutrients (Ward et al. 2011), or prey and irradiance (Rothhaupt 1996; Fischer et al. 2017; Hsu et al. 2022), or all three resources (Berge et al. 2016; Edwards 2019). Because competition tends to suppress prey concentrations, as well as nutrient concentrations under sufficient irradiance, the relevant parameter space for considering competitive outcomes may generally be the low-concentration region favorable to mixotrophs. Conversely, the relative performance of heterotrophs may be greatest under non-equilibrium conditions where prey concentration is transiently high, such as episodic blooms or particle-associated microbial hotspots. High mortality rates in productive ecosystems may also benefit heterotrophs, as the top-down control of flagellate populations will mitigate prey depletion and cause competitive outcomes to be driven more by maximum ingestion and growth rates (Fischer et al. 2017).

The trait differences summarized in Fig. 4a imply that if mixotrophic and heterotrophic flagellates are equally abundant in an ecosystem, substantially less prey biomass will flow through mixotrophs, as a result of the latter's substantially lower per capita ingestion rates. At the same time, mixotrophs exhibit greater growth efficiency on average (Fig. 3), which is expected because they can meet some, or potentially all, of their energy demand through absorbed light rather than respiration of prey biomass. If we combine the average differences in ingestion traits with the average difference in growth efficiency, and assume for illustration that dissolved nutrients do not contribute significantly to mixotroph growth, then we can project the growth vs. prey relationship for the average heterotroph and mixotroph (Fig. 4b). Because the mixotroph

disadvantage in  $C_{\max}$  is very similar to the mixotroph advantage in growth efficiency, the predicted growth rates under non-saturating prey concentrations are similar for mixotrophs and heterotrophs. In terms of ecosystem fluxes, this suggests that mixotrophs could consume a much smaller fraction of total prey, but still transfer the same total amount of energy and nutrients from prey to higher trophic levels, compared to heterotrophs. Differences in mixotroph and heterotroph physiology could also affect in situ estimates of grazing contributions, because short-term uptake of labeled prey cells may reflect differences in ingestion rates, while longer-term incorporation of labeled biomass may reflect both ingestion and assimilation differences (Hartmann et al. 2012). In terms of competitive interactions, Fig. 4b suggests that a tradeoff between clearance rate and growth efficiency may equalize the fitness of competing strategies, which may help explain the widespread co-occurrence of mixotrophic and heterotrophic flagellates in sunlit waters. Incorporation of these trait differences and trait variation into ecosystem models may help constrain the many potential ecosystem impacts of mixotrophy (Ward and Follows 2016; Leles et al. 2018; Glibert and Mitra 2022).

As stated in the “Results” section, the differences in growth efficiency reported here should be treated with caution. Efficiencies were calculated based on cell biovolumes, rather than elemental or energetic transfer efficiencies, and any contribution of dissolved nutrients to biomass synthesis in mixotrophs will bias their calculated efficiency upwards. The high mixotroph growth efficiencies observed in our previous study, where dissolved nitrogen was not supplemented, suggest that the qualitative conclusions from Fig. 4 are robust, but it is still possible that the scarce dissolved nitrogen present in oligotrophic seawater medium contributed to growth. Future work should aim to compare growth efficiencies of diverse mixotrophs and heterotrophs in units of carbon, nutrients, or energy, under uniform conditions, with approaches that minimize or quantify assimilation of nutrients from sources other than prey biomass.

### Underlying mechanisms and allometric scaling

The physical mechanisms underlying functional trait variation among flagellates are not well understood, but the patterns of trait variation documented here may provide some insights. The negative correlation between specific  $C_{\max}$  and growth efficiency is consistent with one previously documented for small mixotrophs from diverse taxa, some of which are included in the current analysis. It has also been found that mixotrophs with a faster growth rate under phototrophic growth conditions (dissolved nutrients but no added prey) tend to have a lower specific clearance rate (Edwards et al. 2023). These multiple lines of evidence imply a spectrum of trophic strategies including autotrophs, mixotrophs ranging from relatively autotrophic to relatively heterotrophic strategies, and heterotrophs. The mechanism causing lower specific

$C_{\max}$  of mixotrophs relative to heterotrophs, as well as variation along the spectrum of mixotrophs, is not clear, but  $C_{\max}$  is thought to be driven by the flagellar mechanics which affect encounter rates between predator and prey (Nielsen and Kiørboe 2021). Therefore, varying investment in swimming speed and other aspects of feeding current generation may underlie variation in  $C_{\max}$ . An increase in cell size driven by the inclusion of one or more chloroplasts will also reduce the volume-specific clearance rate, all else equal (Raven 1997; Berge *et al.* 2016). Within heterotrophic flagellates there is also a (weaker) negative correlation between specific  $C_{\max}$  and growth efficiency, which suggests additional trait covariation not related to phototrophy vs. phagotrophy. One possibility is a fast-slow axis of metabolic strategies, where higher ingestion rates are driven by higher metabolic rates that reduce growth efficiency, and potentially cause higher encounter rates with predators as well (Kiørboe and Thomas 2020).

The greater mixotroph penalty for  $I_{\max}$  vs.  $C_{\max}$  implies these traits have distinct mechanistic underpinnings. Maximum ingestion rate is expected to be limited by the time it takes to handle and ingest prey (Suzuki *et al.* 2021), or by the time it takes to digest prey (Jeschke *et al.* 2002). These processes may be more energetically expensive than the flagellar motion driving  $C_{\max}$  (Raven and Lavoie 2021), which could lead to a greater reduction in  $I_{\max}$  when mixotrophs invest energy in phototrophy instead of phagotrophy. The inclusion of relatively bulky photosynthetic machinery in the cell could also reduce the maximum digestion rate by reducing the number of prey that can be simultaneously digested. Finally, because prey concentrations are generally dilute and non-saturating in pelagic systems, mixotrophs are likely under greater selection to increase  $C_{\max}$  compared to  $I_{\max}$ .

Similar to the patterns revealed here, previous compilations of heterotrophic pelagic organisms, including unicellular and multicellular life, have also found relatively uniform allometric relationships across taxa for  $I_{\max}$ , but distinct intercepts for  $C_{\max}$  (Hansen *et al.* 1997; Kiørboe and Hirst 2014). These patterns imply that the efficiency of prey encounter relative to cell size declines fairly steeply as cell size increases, but that dinoflagellates have an innovation that increases their baseline encounter rate. A possible contributor is that dinoflagellates possess ingestion mechanisms allowing them to ingest relatively large prey (Jeong *et al.* 2010), which should increase contact rates (Shimeta 1993). In this dataset the geometric mean predator : prey size ratio (using equivalent spherical diameter) is 1.5 for dinoflagellates and 4.5 for non-dinoflagellates.

Allometric scaling of ecophysiological rates is often quantified by a power law function of body mass ( $M$ ), and whole organism energy consumption often scales proportional to  $M^{3/4}$ , which is equivalent to  $M^{-1/4}$  scaling for mass-specific energy consumption (Brown *et al.* 2004). Other physiological and ecological rates can exhibit quarter-power scaling as well, presumably because they are driven by rates of energy consumption (Brown *et al.* 2004). The scaling exponent for  $C_{\max}$

in the current study is substantially shallower than 0.75, being 0.38 with a 95% CI of (0.19, 0.58). In contrast,  $I_{\max}$  has a steeper exponent of 0.84 with 95% CI of (0.67, 1.0), overlapping 0.75. Importantly, we analyzed both of these traits as a function of cell volume, rather than cell mass. Cell mass was measured in very few of the compiled experiments, but among protists the mass per volume tends to decline with increasing cell size, such that  $M \sim V^b$ , with relevant estimates of  $b$  ranging from 0.86 (dinoflagellates only) to 0.94 (all non-diatom protists) (Menden-Deuer and Lessard 2000). If we extrapolate mass scaling relationships for  $C_{\max}$  and  $I_{\max}$  using a mass–volume scaling exponent of 0.94 then  $C_{\max}$  would scale with cell mass with an exponent of 0.40, and  $I_{\max}$  with an exponent of 0.89. If we use a shallower mass–volume scaling exponent of 0.86 then the predicted exponents are 0.43 for  $C_{\max}$  and 0.96 for  $I_{\max}$ . It is noteworthy that the shallower  $C_{\max}$  scaling only occurs when recognizing that dinoflagellates and non-dinoflagellates have similar within-group slopes but different intercepts (Fig. 1). If all flagellates are pooled (i.e., distinct intercepts ignored), then  $C_{\max}$  scales with cell volume with an exponent of 0.78, and is predicted to scale with cell mass with exponents ranging from 0.83 to 0.89, which is similar to  $I_{\max}$ . Therefore, when considering flagellates as a whole, the ingestion rates at both low and high prey concentrations scale with cell volume in a way that may be consistent with quarter-power scaling but is somewhat closer to isometric scaling.

## Conclusion

Our results suggest that the average mixotrophic flagellate ingests prey at a substantially lower rate than the average heterotrophic flagellate, although this penalty is reduced by half under low prey concentrations. The greater growth efficiency of mixotrophs, facilitated by sunlight, may be large enough to yield a prey-supported growth rate equivalent to heterotrophs at typical prey concentrations, even when ingestion is much slower. The tradeoff between ingestion rate and growth efficiency appears to occur broadly across mixotrophs as well, and to a lesser extent across heterotrophs, illuminating a broad spectrum of flagellate trophic strategies that may correlate with environmental gradients. Dinoflagellates and other flagellate species exhibit similar constraints on trait variation, but dinoflagellates achieve a much higher clearance rate than would be expected for a particular cell size, which may underlie their success among the larger unicellular plankton. Future efforts to further refine our understanding of the tradeoffs that govern competition among phototrophic, mixotrophic, and heterotrophic marine flagellates would benefit from comparative studies using more isolates of all types from the open ocean—including mass or energy-based measurements of growth efficiencies—along with application of methods to discriminate and quantify *in situ* carbon and energy fluxes through mixotrophic and heterotrophic consumers.

## Data availability statement

All data and R code for data analysis are provided in Supporting Information.

## References Cited

Arndt, H., D. Dietrich, B. Auer, E.-J. Cleven, T. Grafenhan, M. Weitere, and A. P. Mylnikov. 2000. Functional diversity of heterotrophic flagellates in aquatic ecosystems, p. 240–268. In B. S. C. Leadbeater and J. C. Green [eds.], *The flagellates*. Taylor & Francis Ltd.

Azam, F., D. C. Smith, G. F. Steward, and Å. Hagström. 1994. Bacteria-organic matter coupling and its significance for oceanic carbon cycling. *Microb. Ecol.* **28**: 167–179.

Berge, T., S. Chakraborty, P. J. Hansen, and K. H. Andersen. 2016. Modeling succession of key resource-harvesting traits of mixotrophic plankton. *ISME J.* **11**: 212–223.

Bolker B, and R Development Core Team. 2022. *bbmle*: Tools for general maximum likelihood estimation. R package version 1.0.25. Available from <https://CRAN.R-project.org/package=bbmle>

Brooks, M., and others. 2022. *glmmTMB*: Generalized linear mixed models using template model builder.

Brown, J. H., J. F. Gillooly, A. P. Allen, V. M. Savage, and G. B. West. 2004. Toward a metabolic theory of ecology. *Ecology* **85**: 1771–1789.

Edwards, K. F. 2019. Mixotrophy in nanoflagellates across environmental gradients in the ocean. *Proc. Nat. Acad. Sci. U.S.A.* **116**: 6211–6220.

Edwards, K. F., Q. Li, K. A. McBeain, C. R. Schvarcz, and G. F. Steward. 2023. Trophic strategies explain the ocean niches of small eukaryotic phytoplankton. *Proc. Royal Soc. B* **290**. doi:10.1098/rspb.2022.2021

Fischer, R., H. Giebel, H. Hillebrand, and R. Ptacnik. 2017. Importance of mixotrophic bacterivory can be predicted by light and loss rates. *Oikos* **126**: 713–722.

Glibert, P. M., and A. Mitra. 2022. From webs, loops, shunts, and pumps to microbial multitasking: Evolving concepts of marine microbial ecology, the mixoplankton paradigm, and implications for a future ocean. *Limnol. Oceanogr.* **67**: 585–597.

Hansen, P. J., P. K. Bjørnsen, and B. W. Hansen. 1997. Zooplankton grazing and growth: Scaling within the 2–2000  $\mu\text{m}$  body size range. *Limnol. Oceanogr.* **42**: 687–704.

Hartmann, M., C. Grob, G. A. Tarran, A. P. Martin, P. H. Burkhill, and D. J. Scanlan. 2012. Mixotrophic basis of Atlantic oligotrophic ecosystems. *Proc. Nat. Acad. Sci. U.S.A.* **109**: 5756–5760.

Holling, C. S. 1966. The functional response of invertebrate predators to prey density. *Mem. Entomol. Soc. Can.* **98**: 5–86.

Hsu, V., F. Pfab, and H. V. Moeller. 2022. Niche expansion via acquired metabolism facilitates competitive dominance in planktonic communities. *Ecology* **103**: e3693.

Jeong, H. J., Y. Du Yoo, J. S. Kim, K. A. Seong, N. S. Kang, and T. H. Kim. 2010. Growth, feeding and ecological roles of the mixotrophic and heterotrophic dinoflagellates in marine planktonic food webs. *Ocean Sci. J.* **45**: 65–91.

Jeschke, J. M., M. Kopp, and R. Tollrian. 2002. Predator functional responses: Discriminating between handling and digesting prey. *Ecol. Monogr.* **72**: 95–112.

Kiørboe, T. 2008. A mechanistic approach to plankton ecology. Princeton Univ. Press.

Kiørboe, T., and A. G. Hirst. 2014. Shifts in mass scaling of respiration, feeding, and growth rates across life-form transitions in marine pelagic organisms. *Am. Nat.* **183**: E118–E130.

Kiørboe, T., and M. K. Thomas. 2020. Heterotrophic eukaryotes show a slow-fast continuum, not a gleaner-exploiter trade-off. *Proc. Nat. Acad. Sci. U.S.A.* **117**: 24893–24899.

Leles, S. G., L. Polimene, J. Bruggeman, J. Blackford, S. Ciavatta, A. Mitra, and K. J. Flynn. 2018. Modelling mixotrophic functional diversity and implications for ecosystem function. *J. Plankton Res.* **40**: 627–642.

Li, Q., K. F. Edwards, C. R. Schvarcz, K. E. Selph, and G. F. Steward. 2021. Plasticity in the grazing ecophysiology of *Florenciella* (Dichyochophyceae), a mixotrophic nanoflagellate that consumes *Prochlorococcus* and other bacteria. *Limnol. Oceanogr.* **66**: 47–60.

Lindemann, C., Ø. Fiksen, K. H. Andersen, and D. L. Aksnes. 2016. Scaling laws in phytoplankton nutrient uptake affinity. *Front. Mar. Sci.* **3**: 26.

Logares, R., S. Audic, S. Santini, M. C. Pernice, C. de Vargas, and R. Massana. 2012. Diversity patterns and activity of uncultured marine heterotrophic flagellates unveiled with pyrosequencing. *ISME J.* **6**: 1823–1833.

Menden-Deuer, S., and E. J. Lessard. 2000. Carbon to volume relationships for dinoflagellates, diatoms, and other protist plankton. *Limnol. Oceanogr.* **45**: 569–579.

Mitra, A., A. Calbet, and M. Zubkov. 2014. The role of mixotrophic protists in the biological carbon pump. *Biogeosciences* **11**: 995–1005.

Mitra, A., and others. 2016. Defining planktonic protist functional groups on mechanisms for energy and nutrient acquisition: Incorporation of diverse mixotrophic strategies. *Protist* **167**: 106–120.

Nielsen, L. T., and T. Kiørboe. 2021. Foraging trade-offs, flagellar arrangements, and flow architecture of planktonic protists. *Proc. Nat. Acad. Sci. U.S.A.* **118**: e2009930118.

Pierella Karlusich, J. J., F. M. Ibarbalz, and C. Bowler. 2020. Phytoplankton in the Tara Ocean. *Annu. Rev. Mar. Sci.* **12**: 233–265.

Raven, J. 1997. Phagotrophy in phototrophs. *Limnol. Oceanogr.* **42**: 198–205.

Raven, J. A., and M. Lavoie. 2021. Movement of aquatic oxygenic photosynthetic organisms. *In Progress in botany*. Springer. doi:[10.1007/124\\_2021\\_55](https://doi.org/10.1007/124_2021_55)

Rothhaupt, K. O. 1996. Laboratory experiments with a mixotrophic chrysophyte and obligately phagotrophic and phototrophic competitors. *Ecology* **77**: 716–724.

Shimeta, J. 1993. Diffusional encounter of submicrometer particles and small cells by suspension feeders. *Limnol. Oceanogr.* **38**: 456–465.

Smalley, G. W., D. W. Coats, and D. K. Stoecker. 2003. Feeding in the mixotrophic dinoflagellate *Ceratium furca* is influenced by intracellular nutrient concentrations. *Mar. Ecol. Prog. Ser.* **262**: 137–151.

Stoecker, D. K. 1998. Conceptual models of mixotrophy in planktonic protists and some ecological and evolutionary implications. *Eur. J. Protistol.* **290**: 281–290.

Stoecker, D. K., P. J. Hansen, D. A. Caron, and A. Mitra. 2017. Mixotrophy in the marine plankton. *Annu. Rev. Mar. Sci.* **9**: 2.1–2.25.

Suzuki, S., A. Andersen, and T. Kiørboe. 2021. Mechanisms and fluid dynamics of foraging in heterotrophic nanoflagellates. *bioRxiv*. doi:[10.1101/2021.04.01.438049](https://doi.org/10.1101/2021.04.01.438049)

Tummers, B. 2006. DataThief III. Available from <https://datathief.org/>

Ward, B. A., S. Dutkiewicz, A. D. Barton, and M. J. Follows. 2011. Biophysical aspects of resource acquisition and competition in algal mixotrophs. *Am. Nat.* **178**: 98–112.

Ward, B. A., and M. J. Follows. 2016. Marine mixotrophy increases trophic transfer efficiency, mean organism size, and vertical carbon flux. *Proc. Nat. Acad. Sci. U.S.A.* **113**: 2958–2963.

### Acknowledgments

This work was supported by NSF grants OCE 15-59356, RII Track-2 FEC 1736030, and DEB 2224832 to GFS and KFE, a Simons Foundation Early Career Award to KFE, and the Young Scientists Fund of the National Natural Science Foundation of China grant 42106097 to QL.

### Conflict of Interest

The authors declare no conflicts of interest.

Submitted 26 August 2022

Revised 18 January 2023

Accepted 05 February 2023

Associate editor: Thomas Kiørboe